AJBAR Vol. 5(1), February 2026: 10-24, ISSN: 2811-2881

Arid Zone Journal of Basic and Applied Research

Faculty of Science, Kashim Ibrahim University
Maiduguri, Nigeria

Journal homepage: https://www.azjournalbar.com

Research Article

Synthesis, Characterization and Biological Evaluation of Ni(II) and Cu(II) Complexes of a Tri-halogenated Asymmetric Tetradentate Schiff Base Ligand

*[1]Abubakar A. Ahmed, [1]Mohammed B. Fugu, [1]Naomi P. Ndahi, [2]Hussaini A. Barma, [1]Ibrahim M. Wakil and [1]Ibrahim Waziri

[1]Department of Pure and Applied Chemistry, Faculty of Physical Sciences, University of Maiduguri, P.M.B. 1069, Maiduguri, Borno State, Nigeria

[2]Department of Chemistry, Kashim Ibrahim University, P. M. B. 1122, Maiduguri, Borno State, Nigeria

***Corresponding author's Email**: abubakarabdullahiahmed28@gmail.com, doi.org/10.55639/607.02010095

ARTICLE INFO:

Keywords:
Asymmetric_Schiff base,
4-chloro-1,2-diaminobenzene,
4-chloro-*o*-phenylenediamine.

ABSTRACT

The growing global menace of antimicrobial resistance and oxidative stress–related disorders have prompted the search for adequate and effective bifunctional molecules that have the proclivity of circumventing the duo. In this work, we synthesized and explored the antioxidant and antimicrobial potency of a Schiff base,2-bromo-4-chloro-6-((E)-((5-chloro-2-((E)-(2-hydroxybenzylidene) amino) nphenylimino)methyl)phenol (H_2L) obtained by condensing 4-chloro-1,2-diaminobenzene, salicylaldehyde and 3-bromo-5-chlorosalicylaldehyde in 1:1:1 molar ratio. The complexes of Ni^{2+} and Cu^{2+} were further synthesized. A comprehensive physicochemical and spectroscopic characterization including elemental analysis, High Resolution Mass Spectrometry (HRMS), ^{1}H and ^{13}C Nuclear Magnetic Resonance (NMR), UV-Visible, and Fourier Transform Infrared (FTIR) Spectroscopy, molar conductance and magnetic susceptibility were performed. The data established the asymmetry of the Schiff base coordinated to the metal centres *via* the azomethine N-atom and phenolic O-atoms, forming four coordinate square planar geometry for both Ni(II) and Cu(II) complexes. Furthermore, bioassay results demonstrated that H_2L showed mild activity against Gram negative bacteria (*Escherichia coli* and *Salmonella Typhi*) and fungus *Candida albicans* as determined by disc diffusion method. By contrast, this compound showed no effect against Gram-positive bacterial species (*Streptococcus aureus* and *Bacillus subtilis*). After complexation, the NiL chelate gained potency against *B. subtilis* with inhibition zone diameter, IZD = 10.00 ± 0.00 mm while the CuL against *S. aureus* and *B. subtilis* with IZD of 12.00 ± 0.00 and 12.00 ± 0.00 mm, respectively. DPPH scavenging potency of these compounds follows the order: CuL > H_2L > NiL with CuL possessed the best efficacy of 98.46% recorded at concentration of 0.5 mg mL^{-1}.

Corresponding author: Abubakar A. Ahmed **Email**: abubakarabdullahiahmed28@gmail.com
Department of Pure and Applied Chemistry, Faculty of Physical Sciences, University of Maiduguri

INTRODUCTION

Although remarkable progresses have been accomplished in antimicrobial therapy, bacterial infections persist as a major global health menace. According to a global review of the year 2022, 7.7 million deaths corresponding to 13.6% of all global fatalities have been linked to bacterial infections (GBD 2019 Antimicrobial Resistance Collaborators, 2022). This fatality rate is further aggravated by the increasing resistance of bacterial strains to antibiotics, which has rendered many conventional treatments ineffective (Ahmed *et al.*, 2024; Rajput *et al.*, 2024). To combat this unpleasant phenomenon, design and development of novel antimicrobial agents have become an utmost research priority with Schiff bases being one-of-a-kind candidates showing great promise. Schiff bases have garnered enormous scientific interest in recent times due to their versatility in therapeutic and biological activities, primarily ascribed to their strong complexation ability and the possession of the azomethine (─CH=N─) functional group (Boulechfar *et al.,* 2023; Mohamed *et al.*, 2025). Plethora of studies have hinted to their potential for drug development especially as antioxidant, antibacterial, and antifungal agents (Russo *et al.*, 2023; Akter *et al.*, 2024; Bhuiyan *et al.*, 2024). From structural view point, Schiff bases are nitrogen analogue of aldehyde or ketone in which the oxygen is substituted by nitrogen atom to form carbon-nitrogen double bond (HC=N) often referred to as azomethine. As versatile ligands in coordination chemistry, they variously bind to metal ions in different oxidation states, leading to metal chelates with enhanced chemical stability and chemotherapeutic activity (Desai *et al.*, 2025).

In recent years, tetradentate Schiff bases derivatives, especially those possessing halogen substituents have demonstrated promising potential as dual-antimicrobial and antioxidant agents (Abdel-Rahman *et al.*, 2022; Gogoi and Barman, 2023). Halogens such as chlorine, bromine, and iodine are known to enhance biological activity through increased lipophilicity and membrane permeability (Kargar *et al.* 2021; Wang *et al.*, 2024; Nthehang *et al.*, 2025).

Although multi-halogen-substituted Schiff base scaffolds have been reported extensively, limited attention has been given to asymmetric Schiff base systems that incorporate multiple halogen substituents within the same molecular scaffold. This offers great advantages by changing the electronic properties making them superior to their symmetrical counterparts inducing enhanced antioxidant and antimicrobial efficacy that can address bacterial resistance and Reactive oxygen species (Nejo *et al.*, 2010; Proetto *et al.,* 2012; Nguyen *et al.,* 2021). Therefore, exploring Schiff bases containing multiple halogen substituents represents a promising strategy in the ongoing development of bifunctional compounds with enhanced antimicrobial and antioxidant efficacy.

We herein, reported asymmetrical Schiff base derived from 4-chloro-1,2-diaminobenzene, salicylaldehyde and 3-bromo-5-chlorosalicylaldehyde, and its Ni(II) and Cu(II) complexes. The ligand and its metal complexes were characterized by analytical and spectroscopic methods and assessed for antimicrobial and antioxidant efficacies.

2.0. EXPERIMENTAL SECTION

2.1. Chemicals and Instruments

Analytical grade (AR) chemicals and solvents were purchased and utilized as received – salicylaldehyde (98%, Merck), 3-bromo-5-chlorosalicylaldehyde (98%, Sigma-Aldrich), 4-chloro-1,2-diaminobenzene (99.5%, Sigma-Aldrich), $NiCl_2.6H_2O$ and $CuCl_2.2H_2O$, ethanol, methanol, dichloromethane, acetonitrile, dimethylformamide and dimethylsulfoxide.

Vario Elementar III microcube CHNS Analyser was employed to perform the elemental analysis. For metal content analyses, Spectro Arcos FSH12 Inductively-coupled Plasma Optical Emission (ICP-OES) Spectrometer was used. FT-IR spectra were run on a Nicolet iS5 FT-IR Spectrometer with an iD7 attachment at the range of 4000-400 cm^{-1}. Bruker-500 MHz Spectrometer (500 MHz for ^1H and 125 MHz for ^{13}C) was used to obtain the ^1H and ^{13}C NMR spectra of the unsymmetrical Schiff bases ligands using DMSO-d_6 as a solvent and TMS as a reference. Mass spectra was recorded on a high-resolution mass spectrometry Waters Acquity UPLC Synapt G2HD machine. Room temperature magnetic susceptibility measurements was executed on a Sherwood MK1 Magnetic susceptibility balance with $Hg[Co(SCN)_4]$ as standard. Conductivities of 10^{-3} M solution of the complexes were

measured in DMSO at 25 °C using a Hand-Held MP 33 Conductivity Meter.

2.2. Synthesis of the Schiff Base Ligand, 2-bromo-4-chloro-6-((E)-((5-chloro-2-((E)-(2-hydroxybenzylidene) amino)phenylimino)methyl)phenol (H_2L)

The synthesis was performed by one-pot condensation between 4-chloro-1,2-diaminobenzene (0.29 g, 2 mmol), salicylaldehyde (0.21 mL, 2 mmol) and 3-bromo-5-chlorosalicylaldehyde (0.47 g, 2 mmol) each in 15 mL of ethanol as previously described for similar synthesis (Priya *et al.*, 2024; Akbari *et al.*, 2024). The reaction was magnetically stirred for 5 h at room temperature. The precipitate formed was filtered, washed with ethanol and methanol, and vacuum dried. A dark orange solid was obtained and subjected to characterization.

H_2L; Colour: Dark orange, Yield: 0.50 g, 53.86%. M. p: 271 °C. M. W.: 464.14 $gmol^{-1}$. Anal. Calcd for $C_{20}H_{13}BrCl_2N_2O_2$: C, 51.75%; H, 2.82%; N, 6.04%. Found: C, 51.45%; H, 2.76%; N, 5.98%. ATR-FTIR (cm^{-1}): 3066.86 (O–H), 1610.34 (C=N), 1204.36 (C–O). ^{1}H NMR (500 MHz, DMSO-*d6*), δ (ppm): 13.811 (s, 1H, OH^{1}), 13.614 (s, 1H, OH^{20}), 9.002 (s, 1H, ^{7}HC=N), 8.973 (s, 1H, ^{14}HC=N), 7.786 (s, 1H, Ar-H^{5}), 7.782 (s, 1H, Ar-H^{3}), 7.843 (s, 1H, Ar-H^{19}), 7.817 (s, 2H, Ar-$H^{9,11}$), 7.782 – 7.339 (m, other Ar-H). ^{13}C-NMR (125 MHz, DMSO-*d6*), δ (ppm)): δ 164.19 (^{7}C, HC=N), 163.41 (^{14}C, HC=N), 156.52 (^{1}C, C–OH), 156.41 (^{20}C, C–OH), 142.13–111.33 (Ar-C). HR-MS (*m/z*): 462.9617 $[M + H]^+$ (Cal. 462.9616).

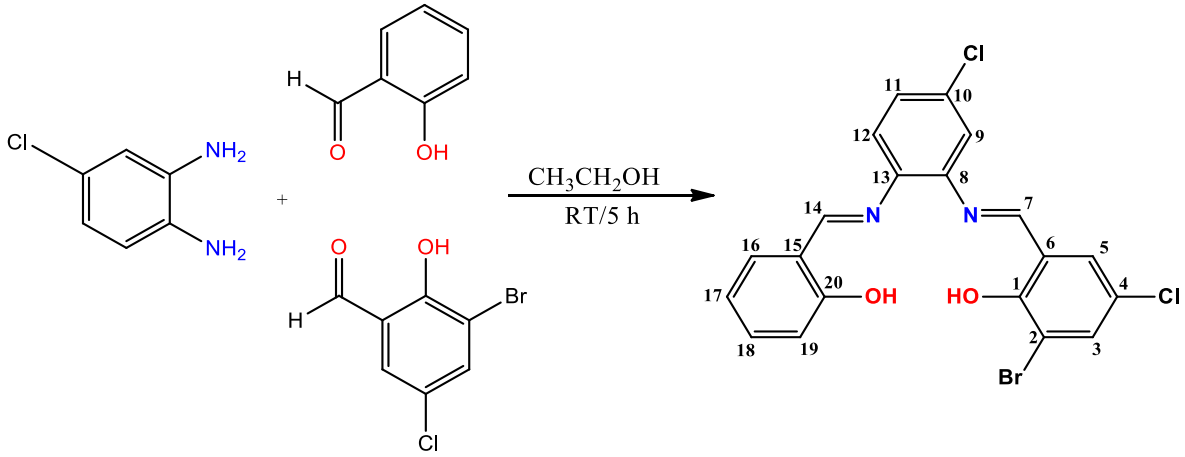

Scheme 1: Synthetic path for the unsymmetrical Schiff base ligand H_2L and atoms numbering

2.3. Synthesis of Metal(II) Complexes

A mixture of methanolic solution (5 mL) of the metal salt ($NiCl_2.6H_2O$: 0.3 mmol, 0.07 g); $CuCl_2.2H_2O$: 0.3 mmol, 0.05 g) and tetrahydrofuran solution (10 mL) of the Schiff base ligand H_2L (0.3 mmol, 0.15 g) in 1:1 molar ratio was stirred under reflux for 4 h, whereupon the precipitate formed thereof was filtered off, washed with methanol, dried and weighed to calculate the % yield (Mohapatra *et al.*, 2024). The general reaction protocol is depicted in Scheme 2.

NiL: Colour: Reddish brown, Yield: 0.16 g, 96%. Dec. Temp.: > 350 °C, M. W.: 520.82 $gmol^{-1}$. Anal. Calcd for $[C_{20}H_{11}BrCl_2N_2O_2Ni]$: C, 46.12%; H, 2.13%; N, 5.38%, Ni, 11.27%. Found: C, 46.06%; H, 2.10%; N, 5.27%, Ni, 11.26%. ATR-FTIR (cm^{-1}): 1599.10 (C=N), 1224.07 (C–O), 432.04 (Ni–O), 406.08 (Ni–N). Ω (DMSO) $Scm^2\ mol^{-1}$: 0.0. μ (B. M.): 2.91.

CuL: Colour: Dark green, Yield: 0.12 g, 98.12%. Dec. Temp.: 248 °C, M. W.: 525.67 $gmol^{-1}$. Anal. Calcd for $[C_{20}H_{11}BrCl_2N_2O_2Cu]$: C, 45.70%; H, 2.11%; N, 5.33%, Cu, 12.09%. Found: C, 45.63%; H, 2.04%; N, 5.26%, Cu, 12.02%. ATR-FTIR (cm^{-1}): 3262.13 (O-H), 1654.82 (C=N), 1243.39 (C–O), 428.09 (Cu–O), 412.27 (Cu–N). Ω (DMSO) $Scm^2\ mol^{-1}$: 0.008. μeff (B. M.): 2.14.

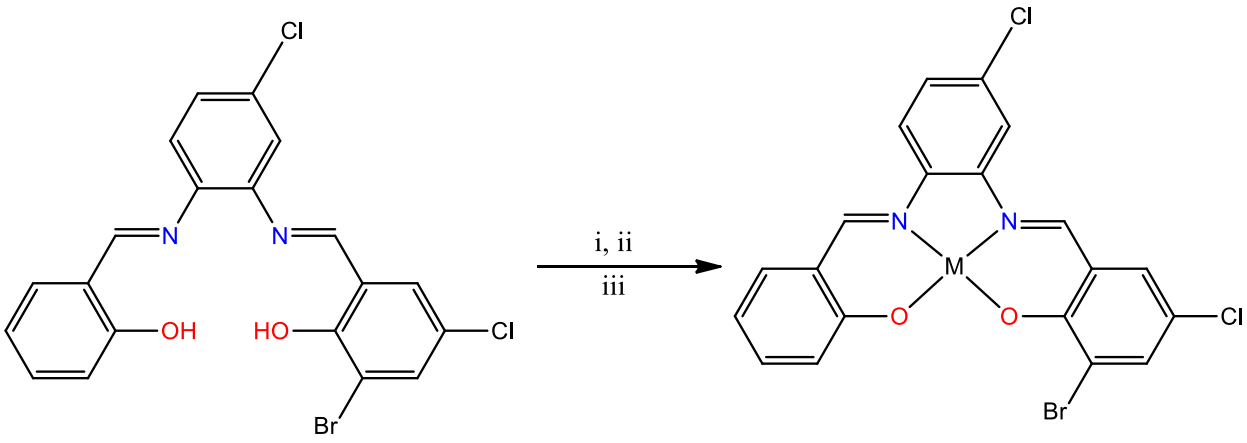

Scheme 2: Synthesis of metal(II) complexes; i = CH_3COH/THF, ii = $NiCL_2.6H_2O$ or $CuCl_2.2H_2O$, iii = 70 ºC, 4 h; M = Cu(II) or Ni(II)

2.4. Antimicrobial Evaluation

The antimicrobial efficacies of the ligand and complexes were evaluated using the disc diffusion method. Paper discs concentrated with 10 µg/mL, 20 µg/mL and 30 µg/mL of the compounds in DMSO were utilized against *Staphylococcus aureus, Bacillus subtilis, Escherichia coli* and *Salmonella Typhi.* Agar plates were prepared and inoculated with 0.1% inoculum suspensions of the test organisms. The plates were then incubated at 37 ºC for 24 h, after which the antibacterial activity was evaluated by measuring the diameter of the inhibition zones around the disc. Results were compared with ciproflaxacin-positive and DMSO-negative controls. Fluconazole and DMSO were used as the positive and negative controls respectively, for antifungal activity evaluation against *Candida albicans* and *Aspergillus fumigatus*. The test organisms were cultured in sterile nutrient broth and incubated for 25–48 h. Sterile Mueller-Hinton agar plates were prepared and inoculated with 0.1% inoculum suspensions of *Candida albicans* and *Aspergillus fumigatus*. The plates were then incubated at 37 ºC for 24 h, after which the antifungal activity was assessed by measuring the diameter of the inhibition zones around the wells. Results were compared with the positive and negative controls. Simple inhibition zones were estimated in mm and the percentage activity index was calculated using Equation (1) (Juyal *et al.*, 2024).

$$\text{Activity Index (AI)} = \frac{\text{Inhibition zone of test compound (mm)}}{\text{Inhibition zone of standard drug (mm)}} \times 100\% \qquad (1)$$

2.5. Antioxidant Assay

The 2,2-diphenyl-1-picrylhydrazyl (DPPH) free radical scavenging method (Es-Sounni *et al.* 2024). In a nutshell, 1.5 mL of each test compound in dimethylformamide at concentrations of 1, 0.5, 0.25 and 0.125 mg mL^{-1} was added to 1 mL of the ethanolic solution of DPPH (24 mg/L). The mixture was incubated for 30 minutes in darkness at room temperature. Thence, the absorbance of the mixture was recorded at 517 nm against a blank using a UV-Visible spectrophotometer. Ascorbic acid was used as a standard reference. The % DPPH scavenging activity of the test compounds was computed using Equation (2) (Priya *et al.*, 2024). The inhibitory concentration needed to achieve 50% of the maximum scavenging activity known as the IC_{50} value was computed using the linear regression plot of the concentrations of test compounds against % DPPH scavenging activity (Juyal *et al.*, 2024).

$$\%\ \text{DPPH scavenging} = \frac{A_0 - A}{A_0} \times 100\% \qquad (2)$$

where, A and A_0 are the absorbance of test samples and the control, respectively.

3.0. RESULTS AND DISCUSSION

3.1. Physicochemical Properties

Table 1 presents the data from the elemental analyses, colour, melting temperatures, yields of the compounds, and molar conductance values. A tetradentate ligand H_2L was prepared under room temperature by condensing 4-chloro-1,2-diaminobenzene, salicylaldehyde and 3-bromo-5-chlorosalicylaldehyde at 1:1:1 molar ratio. The

ligand H_2L was produced as brown solid with melting temperature of 271 ^{0}C. The complexes are coloured solid, air-stable at normal temperature with high melting points (NiL > 350 ^{0}C and CuL = 248 ^{0}C), and quantitative yield. The H_2L is soluble in common organic solvents like ethyl acetate, dichloromethane, tetrahydrofuran, dimethylformamide and dimethylsulphoxide. While CuL is soluble in dimethylformamide and dimethylsulphoxide, NiL is only slightly soluble in both and insoluble in most common organic solvents. Molar conductance values of the complexes were circa 0.00 S cm^2mol^{-1}, which adequately confirmed the non-electrolytic nature of the chelates (Geary, 1971; Nasaruddin *et al.* 2022). The calculated and observed elemental analysis for H_2L and its chelates were in excellent accordance and revealed that the stoichiometry of the chelates correspond to 1:1 metal-to-ligand.

Table 1: Physicochemical Characteristics of H_2L and its Metal(II) Complexes

Compounds	M.F (M.W)	Colour	Yield (%)	M.P (^{0}C)	Microanalysis %: Found (Calculated)				ʌm (S cm^2mol^{-1})
					C	H	N	M	
H_2L[3]	$C_{20}H_{13}BrCl_2N_2O_2$ (464.14)	Dark orange	0.50 (53.86)	271	51.45 (51.75)	2.76 (2.82)	5.98 (6.04)	-	-
NiL[3]	$[C_{20}H_{11}BrCl_2N_2O_2Ni]$	Reddish brown	0.16 (96.00)	>350	46.06 (46.12)	2.10 (2.13)	5.27 (5.38)	11.26 (11.27)	0.0
CuL[3]	$[C_{20}H_{11}BrCl_2N_2O_2Cu]$	Dark green	0.16 (95.12)	248*	45.63 (45.70)	2.04 (2.11)	5.26 (5.33)	12.02 (12.09)	0.008

3.2. Characterization

3.2.1. NMR Spectral Study of H_2L

The ^{1}H NMR spectrum of the asymmetric Schiff base H_2L is presented in Figure 1. From the data, the appearance of δ value at 8.973 and 9.002 ppm marked the condensation of the aldehydes and amine to yield the two HC=N functional groups, indicating its asymmetric nature (Srivastava *et al.*, 2021). The higher δ value represents the singlet due to the proton of the substituted salicylaldehyde which appeared more de-shielded as a consequence of the presence of electron withdrawing chlorine atom neighbouring it. The existence of the two distinct phenolic OH protons of the salicylaldehyde and 3-Br-5-Cl-salicylaldehyde rings is seen with the occurrence of singlets at δ values 13.614 and 13.811 ppm respectively, integrated to two protons. These chemical shifts are high due to intramolecular hydrogen bonding of the phenolic proton with the imine nitrogen (N–O···H) (Srivastava *et al.*, 2021; Abbas *et al.*, 2024; Todarwal *et al.* 2024). The presence of aromatic protons is signaled by the presence of merged peaks at 7.339 – 7.886 ppm. Notably, the protons positioned on carbon 5 and 3 resonate at high δ values of 7.886 and 7.872 ppm respectively, due to the electronegative environment around them. The signal at 7.817 ppm integrated to two protons is ascribed to the protons adjacent to the chloro substituent of the phenylenediamine moiety (Abdel-Rahman *et al.*, 2021). Besides, the spectrum displayed signals at δ 2.501 and 3.315 ppm belonging to the solvent DMSO-d_6 and H_2O protons as impurity, respectively (Khandan and Khaleel, 2025).

The ^{13}C NMR spectral data provide a corroboration of the formation of the unsymmetrical ligand H_2L. The spectrum is presented in Figure 2. The signals observed at 164.19 and 163.41 ppm are due to the azomethine carbons C-7 and C-14 respectively, substantiating the asymmetry of the ligand. This was further supported by the two signals featured at 156.52 and 156.41 ppm ascribed to the phenolic carbons positioned at C-1 and C-20, respectively. These range of chemical shifts have earlier been reported by Mousa *et al.* (2024). In both types of carbon, the one with the higher δ value (C-7 and C-1) are featured from the halo-substituted ring due to their high electronegativity. The δ values due to C-5 and C-3 were observed at 142.13 and 139.77 ppm, respectively, while the chloro and bromo substituted carbons were envisioned to display signals at 135.50 and 135.35 ppm, respectively. Another notable signal observed at 132.49 ppm is due to the chloro bearing carbon of the phenylenediamine ring (Todarwal *et al.*, 2024). The signals observed between the range of 131.18 – 111.33 ppm are due to aromatic carbons (Abdel-Rahman *et al.*, 2021).

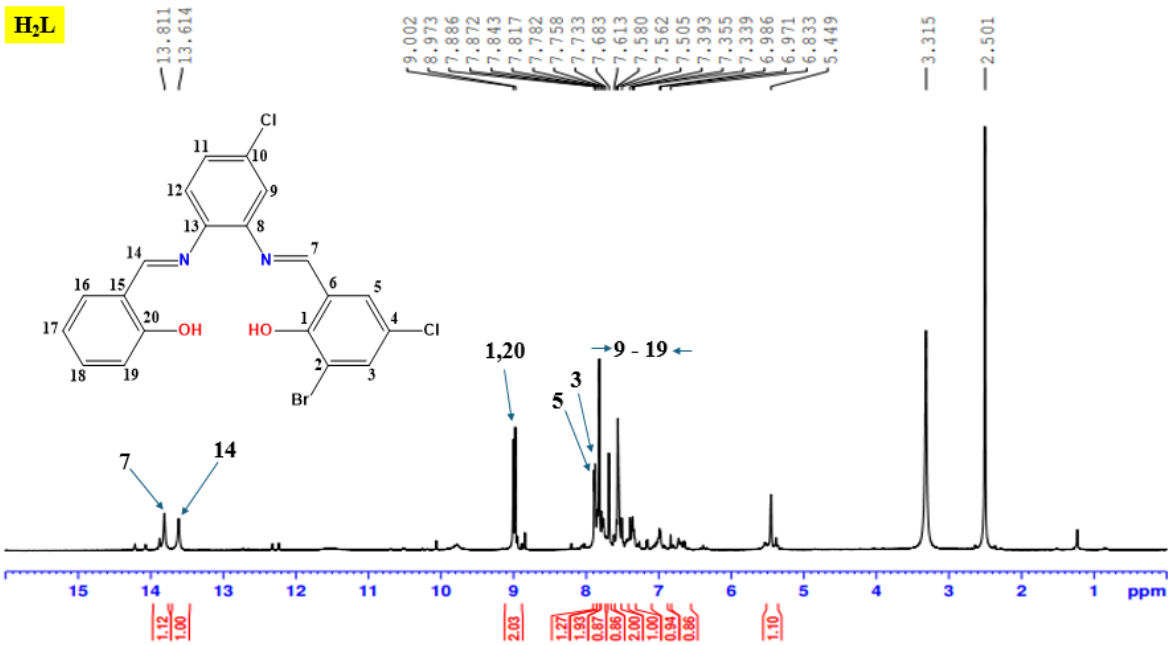

Figure 1: ^{1}H NMR of Ligand H_2L

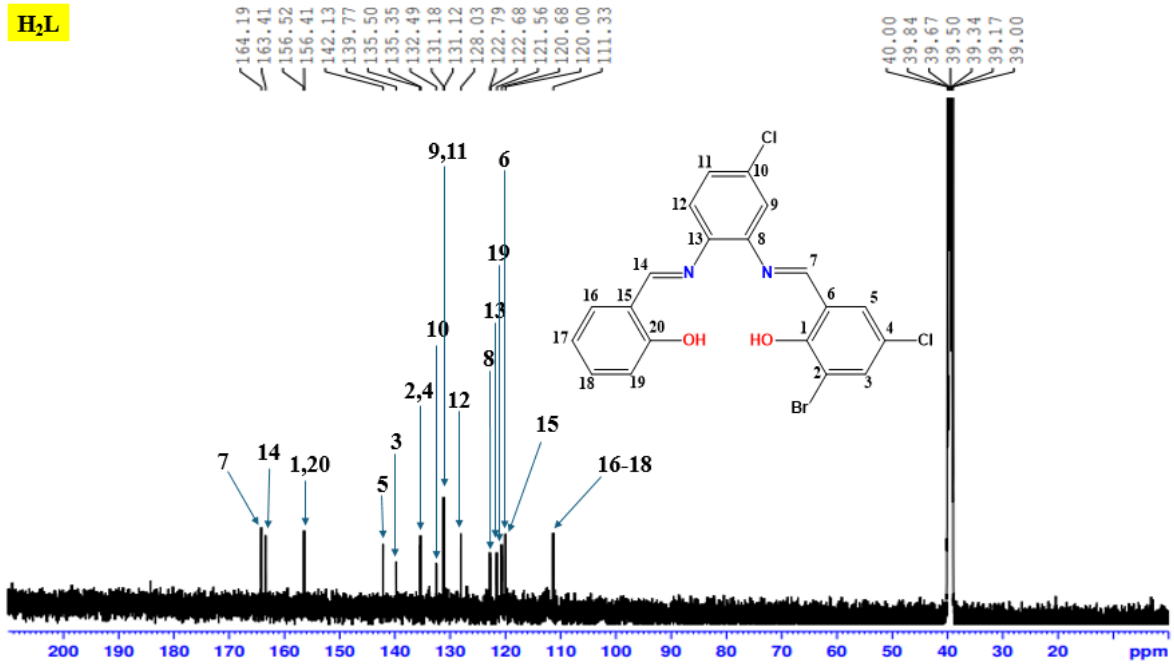

Figure 2: ^{13}C NMR of Ligand H_2L

3.2.2. Mass spectral Analysis of H_2L Ligand

The mass spectrum of the ligand H_2L is presented in Figure 3. The spectrum showed molecular ion peaks at *m/z* = 467.9596, 466.9570, 464.9596 and 462.9617 amu, which were attributed to the $[M+6H]^+$, $[M+5H]^+$, $[M+3H]^+$ and $[M+H]^+$ fragment ions, respectively. These peaks are consistent with calculated values of 467.0007, 466.9929, 464.9772 and 462.9616 amu, respectively (Abd El-Hamid *et al.,* 2021; Sasikumar *et al.*, 2023). The data obtained affirmed the molecular weight of the investigated ligand.

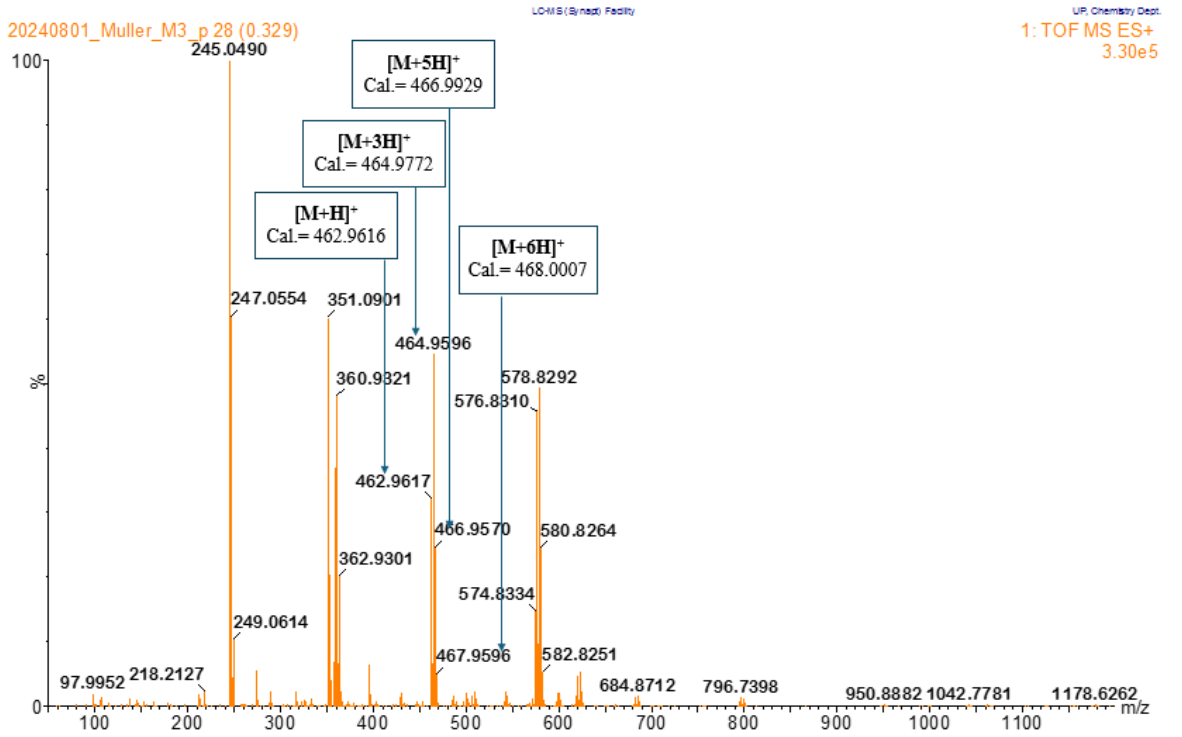

Figure 3: Mass Spectrum of Ligand H_2L

3.2.3. FTIR Spectral Study of H_2L and its Complexes

The infrared spectra of the H_2L and its complexes are presented in Figures 4-6. In the IR spectrum of the unsymmetrical Schiff base ligand, H_2L, the characteristic band attributed to ν(C=N) stretching vibration is featured as strong peak at 1610.34 cm^{-1} (Abdel-Rahman *et al.*, 2021). Upon complexation, this characteristic band due to the azomethine functional group underwent shifts to 1599.10 and 1654.82 cm^{-1} in the spectra of NiL and CuL complexes respectively, indicating participation of nitrogen of ν(C=N) group in the coordination (Nasaruddin *et al.*, 2022; Abbas *et al.*, 2024). For the H_2L, the ν(OH) vibration band of the phenolic group appeared at 3066.86 cm^{-1}, which disappeared upon interaction with Ni(II) ion, indicating deprotonation of the hydroxyl group and subsequent coordination through the oxygen atom. These results agree with the reported results for similar compounds (Torabi *et al.*, 2018). However, CuL complex exhibited broad OH stretching vibration band at 3262.13 cm^{-1} which could be attributed to the moisture in the complex matrix (Peng *et al.,* 2022). Due to coordination to the metal ions through the deprotonated OH, the vibration peaks assignable to ν(C–O) observed at 1204.36 cm^{-1} in H_2L blue shifted to wavenumber 1224.07 and 1243.39 cm^{-1} in NiL and CuL complexes, respectively. Therefore, the C–O bond becomes strengthened upon coordination to the central metals as pointed by the increase in the wavenumber (Kargar *et al.*, 2019). Additionally, two weak Ni–O and Ni–N vibration bands emerged at 432.04 and 406.08 cm^{-1} in the spectrum of the NiL complex. The above feature also occurred in the CuL complex at around 428.09 and 412.27 cm^{-1} due to Cu–O and Cu–N vibration bands, respectively (Abbas *et al.*, 2024; Özbağcı *et al.*, 2024). Conclusively, the spectra revealed that the Ni(II) and Cu(II) atoms coordinated to the unsymmetrical Schiff base ligand, H_2L in N_2O_2 fashion.

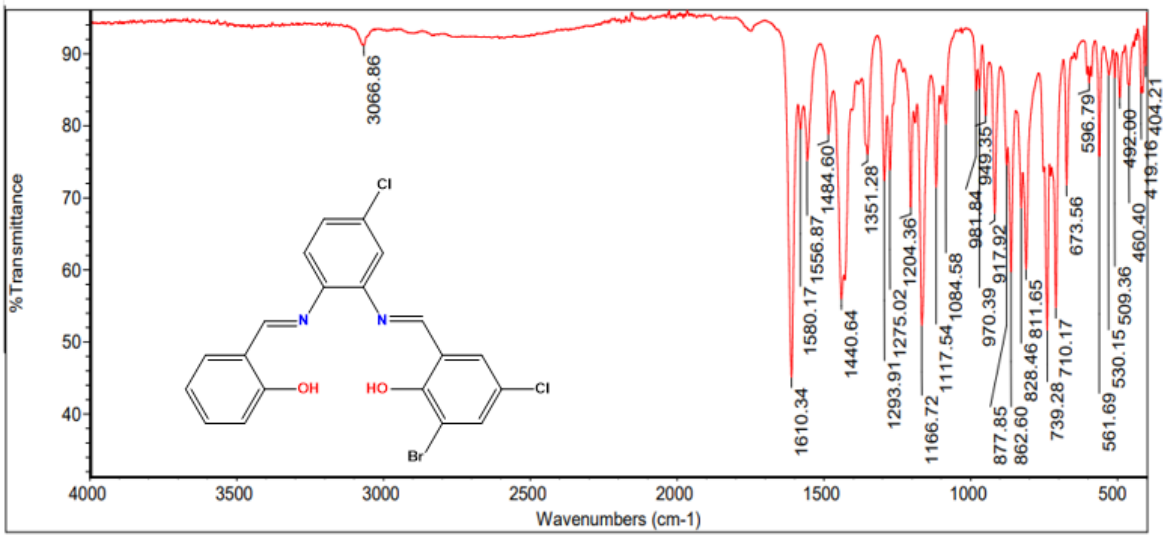

Figure 4: FTIR Spectrum of H_2L

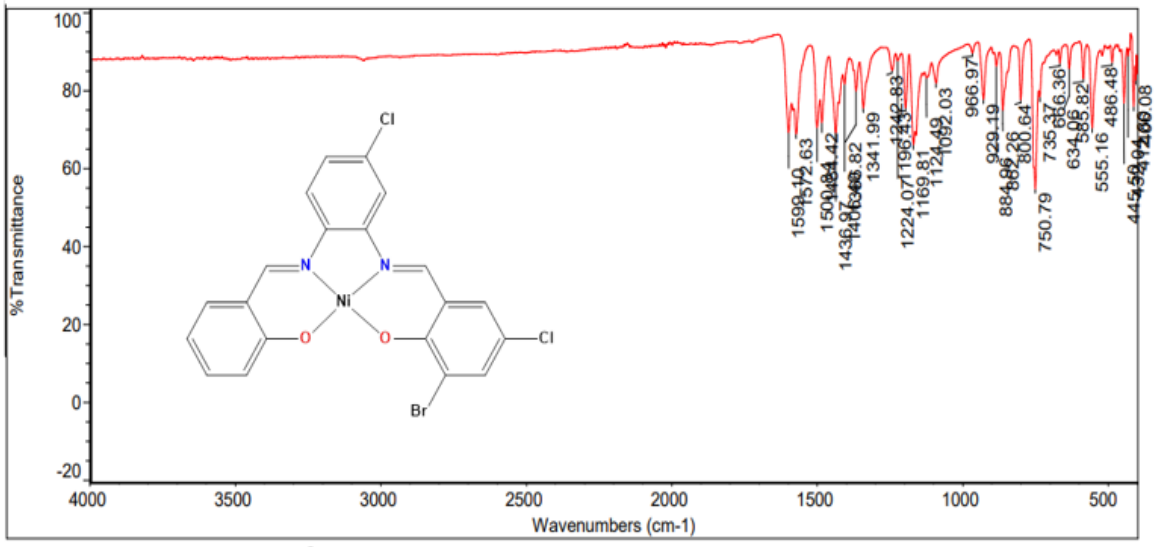

Figure 5: FTIR Spectrum of NiL

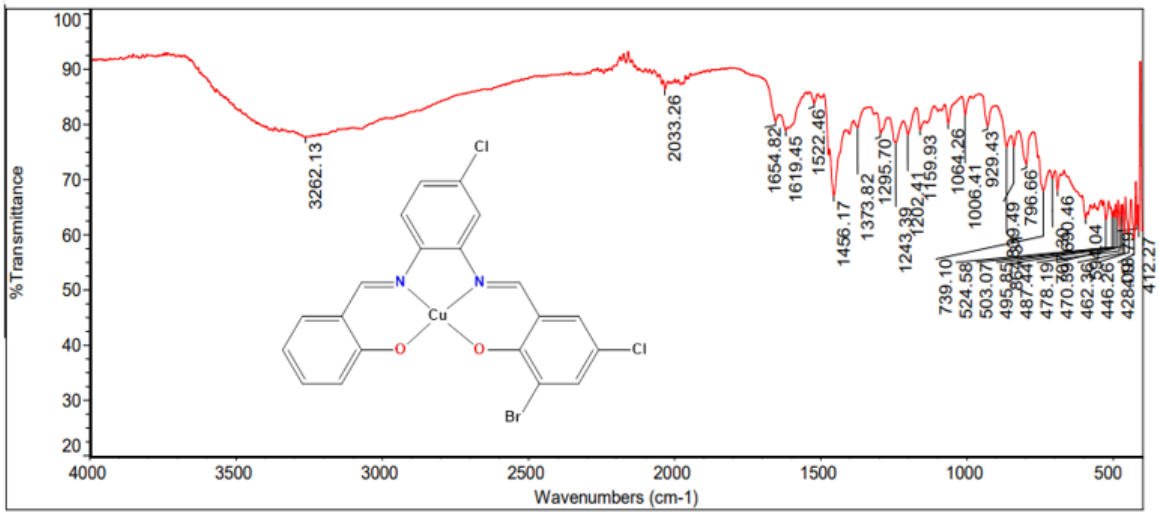

Figure 6: FTIR Spectrum of CuL

3.2.4 UV–Visible absorption spectroscopy and magnetic susceptibility studies

UV–Vis spectra of the free H_2L and its metal chelates (Table 2 and Figures 7–9) were acquired in dimethyl sulfoxide within 200–800 nm. Based on similar compounds, the ligand exhibits three characteristic absorption bands at 315 nm (31,746 cm^{-1}), 340 nm (29,411 cm^{-1}), and 405 nm (24,691 cm^{-1}). The intense bands observed at 315 and 340 nm (ε = 2427 and 2616 $dm^3\ mol^{-1}\ cm^{-1}$, respectively) are attributed to π→π* transitions within the aromatic rings and the azomethine (C=N) chromophore. The lower-energy band at 405 nm (ε = 1260 $dm^3\ mol^{-1}\ cm^{-1}$) is assigned to an n→π* transition involving the lone pair electrons of the azomethine nitrogen and/or phenolic oxygen atoms (Czaplinska *et al.*, 2020; Gacitúa *et al.*, 2022).

The Ni(II) complex (NiL) displays absorption bands at 310 nm (32,258 cm^{-1}), 390 nm (25,641 cm^{-1}), 455 nm (21,978 cm^{-1}), and a weak band at 560 nm (17,857 cm^{-1}). The bands in the ultraviolet and near-visible regions are assigned to ligand-centered π→π* and n→π* transitions, as well as ligand-to-metal charge transfer (LMCT) transitions. The weak band observed at 560 nm with very low molar absorptivity (ε = 11 $dm^3\ mol^{-1}\ cm^{-1}$) is attributed to a d–d transition, characteristic of square planar Ni(II) complexes. The absence of multiple spin-allowed d–d transitions excludes an octahedral geometry. Correspondingly, a magnetic moment of 0 B.M. implies a diamagnetic Ni(II) complex with square planar geometry consistent with the d^8 configuration (Sogukomerogullari *et al.*, 2025).

The electronic spectrum of the Cu(II) complex (CuL) exhibits absorption bands at 305 nm (32,787 cm^{-1}), 380 nm (26,315 cm^{-1}), and a broad band at 460 nm (21,739 cm^{-1}). The higher-energy bands are assigned to ligand-centered transitions, while the band at 460 nm (ε = 126 $dm^3\ mol^{-1}\ cm^{-1}$) is attributed to a d–d transition typical of Cu(II) (d^9) complexes, possibly overlapped with LMCT transitions (Soh *et al.*, 2023). These spectral features are consistent with a square planar geometry around the Cu(II) ion. The observed magnetic moment of 2.14 B.M is higher than spin only value of 1.73 B.M. for d^9 configuration but consistent with square planar geometry.

Table 2: UV–Visible spectral and magnetic susceptibility data

Compounds	Peak		Ɛ	Assignment	μ_{exp}	Geometry
	λ_{max} (nm)	$\bar{\upsilon}$ (cm^{-1})	($dm^3mol^{-1}\ cm^{-1}$)		(B. M.)	
H_2L	315	31,746	2427	π – π* (Aromatic)		
	340	29,411	2616	n – π* (C=N)		
	405	24,691	1260	ILCT		
NiL	310	32,258	279	π – π* (Aromatic)	0	Square planar
	390	25,641	222	n – π* (C=N)		
	455	21,978	162	LMCT		
	560	17,857	11	d-d		
CuL	305	32,787	1678	π – π* (Aromatic)	2.14	Square planar
	380	26,315	1393	n – π* (C=N)		
	460	21,739	126	d-d		

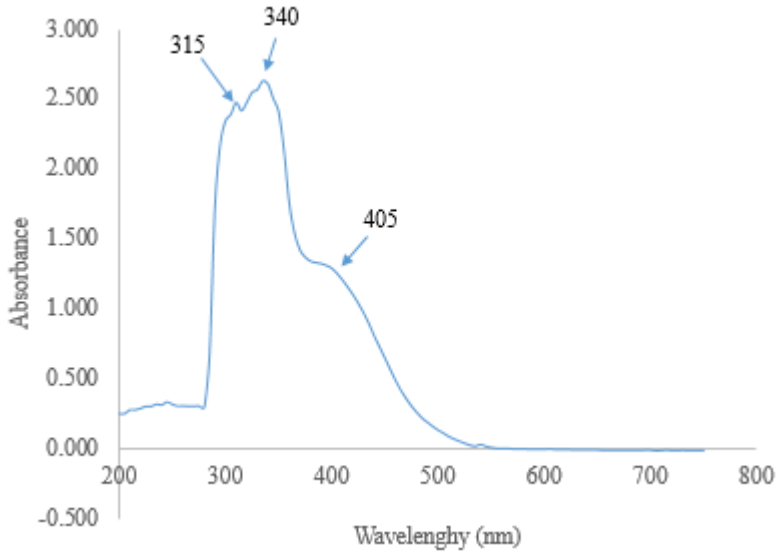

Figure 7: Uv-vis Spectrum of H_2L

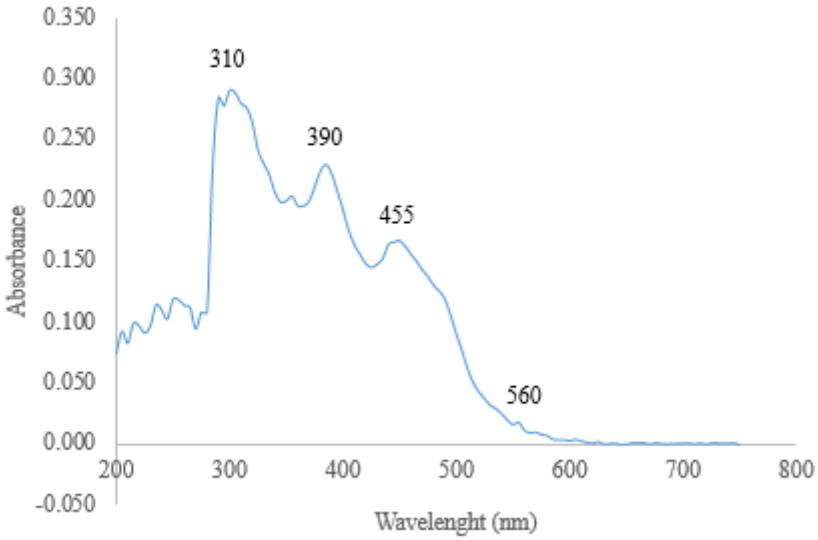

Figure 8: Uv-vis Spectrum of the Complex NiL

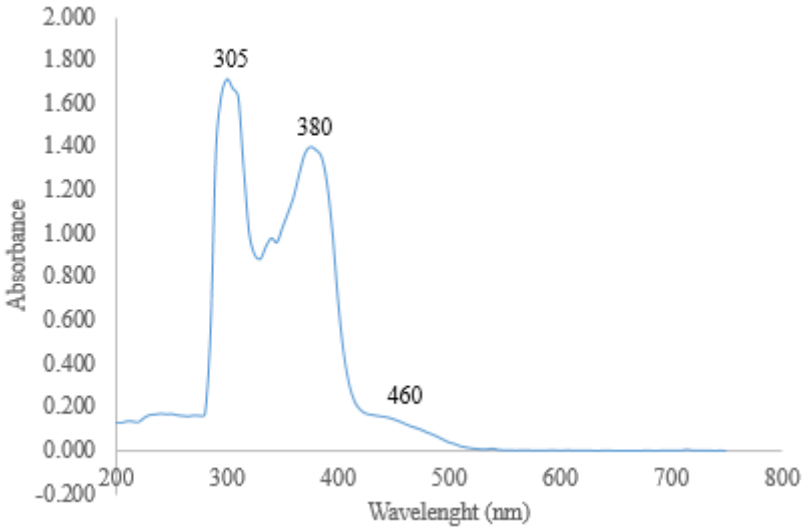

Figure 9: Uv-vis Spectrum of the Complex CuL

3.3. Antimicrobial Activity

The antibacterial and antifungal efficacy of H_2L and its chelates were examined by the disc diffusion method *in vitro* against different strains of Gram positive (*S. aureus* and *B. subtilis*) and Gram negative (*E. coli* and *S. Typi*) bacteria, and fungi (*C. albicans* and *A. fumigatus*). The inhibitory zones of inhibition (IZD) and activity indices are illustrated in Table 3 and Figure 10, respectively. The data for H_2L showed mild activity against Gram negative bacteria (*E. coli* and *S. Typhi*) and fungus *C. albicans* but does not have any against the studied fungus *A. fumigatus* and Gram-positive bacterial species (Ilhan *et al.*, 2014; Vhanale *et al.*, 2019). The potency of the ligand might have arisen from the presence of the electron-withdrawing substituents, azomethine (C=N) and hydroxyl groups (Mohamed *et al.*, 2023). After complexation, the NiL chelate gained potency against *B. subtilis* with IZD = 10.00 ± 0.00 mm while the CuL against *S. aureus* and *B. subtilis* with IZD of 12.00 ± 0.00 and 12.00 ± 0.00 mm, respectively. Furthermore, an enhancement in activity was observed for NiL against *C. albicans*. This enhancement in activity for the chelates could be a subject of the chelation theory (Hijazi *et al.*, 2017). The polarity of the Ni^{2+} and Cu^{2+} got reduced by partial sharing of the their +2 charge with the N and O donor atoms of H_2L ligand and electron delocalization throughout the chelate ring system. This gives rise to lipophilic character of the Ni^{2+} and Cu^{2+} to increase, aiding the permeability of the chelates into lipid membrane layers of the bacterial cell wall, which consequently increases the activity of the chelates and hinder further microorganism growth (Hijazi *et al.*, 2024; Derafa *et al.*, 2024). Overall, the compounds were not as potent as the standard references – ciprofloxacin and fluconazole.

Table 3: Antimicrobial Activity of H_2L and its Metal(II) Complexes

Compounds	Conc. (µg/mL)	*Streptococcus aureus*	*Bacillus subtilis*	*Escherichia coli*	*Salmonella Typhi*	*Candida albicans*	*Aspergillus fumigatus*
H_2L	30	0.00 ± 0.00	0.00 ± 0.00	12.00 ± 0.00	8.00 ± 0.00	13.00 ± 0.00	0.00 ± 0.00
	20	0.00 ± 0.00	0.00 ± 0.00	7.67 ± 0.47	0.00 ± 0.00	9.00 ± 0.00	0.00 ± 0.00
	10	0.00 ± 0.00	0.00 ± 0.00	0.00 ± 0.00	0.00 ± 0.00	0.00 ± 0.00	0.00 ± 0.00
NiL	30	0.00 ± 0.00	10.00 ± 0.00	10.00 ± 0.00	0.00 ± 0.00	15.00 ± 0.00	0.00 ± 0.00
	20	0.00 ± 0.00	7.00 ± 0.00	7.00 ± 0.00	0.00 ± 0.00	11.00 ± 0.00	0.00 ± 0.00
	10	0.00 ± 0.00	0.00 ± 0.00	0.00 ± 0.00	0.00 ± 0.00	7.00 ± 0.00	0.00 ± 0.00
CuL	30	12.00 ± 0.00	13.00 ± 0.00	8.00 ± 0.00	0.00 ± 0.00	10.00 ± 0.00	0.00 ± 0.00
	20	8.00 ± 0.00	8.33 ± 0.47	0.00 ± 0.00	0.00 ± 0.00	7.00 ± 0.00	0.00 ± 0.00
	10	0.00 ± 0.00	0.00 ± 0.00	0.00 ± 0.00	0.00 ± 0.00	0.00 ± 0.00	0.00 ± 0.00
DMSO	30	0.00 ± 0.00	0.00 ± 0.00	0.00 ± 0.00	0.00 ± 0.00	0.00 ± 0.00	0.00 ± 0.00
Ciprofloxacin	30	18.00 ± 0.00	30.00 ± 0.00	23.00 ± 0.00	21.00 ± 0.00	-	-
Fluconazole	30	-	-	-	-	21.00 ± 0.00	25.00±0.00

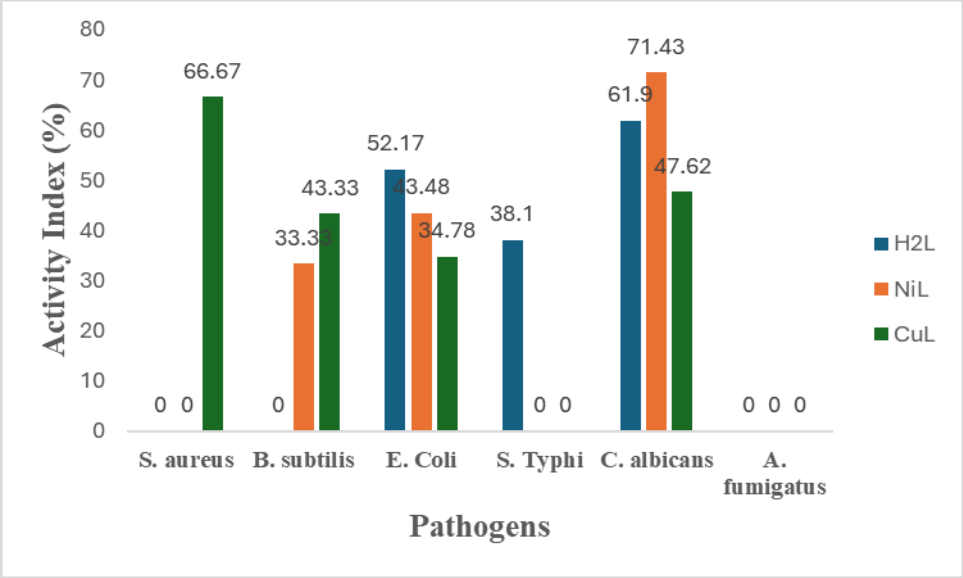

Figure 10: Activity Index (AI) of H_2L and its complexes

3.4. Antioxidant Analysis

The scavenging activities of the H_2L and its chelates obtained by DPPH• free radical scavenging method are presented in Table 4. The H_2L ligand exhibited a scavenging activity ranging between 22.12 and 77.05%, while the metal(II) chelates showed 21.12 – 95.46%. The chelate CuL possessed the best efficacy against free radical with it highest activity of 98.46% recorded at concentration of 0.500 mg mL^{-1}. On the other hand, Ni(II) chelate showed the least potency of 47.20% at the lowest concentration of 0.125 mg mL^{-1} and negative values at higher concentrations. This could be attributed to the fact that the Ni(II) chelate exhibited poor solubility in the test medium which might affect effective interaction of free radicals with the chelate. Essentially, the antioxidant efficacy of a substance is inversely proportional to the IC_{50} value (Singh *et al.*, 2024). Therefore, the potency of these compounds is in the order vitamin C (standard) > CuL > H_2L > NiL with IC_{50} values of 0.004, 0.069, 0.159 and 0.447 mg mL^{-1}, respectively

.

Table 4: Antioxidant Activity of H_2L and its Metal(II) Complexes

Compound	Concentration (mg mL^{-1})				IC_{50} (mg mL^{-1})
	0.125	0.250	0.500	1.000	
	Scavenging activity % Inhibition				
H_2L	77.05	67.65	75.49	22.12	0.159
NiL	47.20	21.12	-41.99	-68.44	0.447
CuL	75.46	84.66	95.46	91.34	0.069
Vitamin C	89.83	91.33	72.72	90.60	0.004

4.0. CONCLUSION

Ni(II) and Cu(II) complexes were generated from a tetradentate asymmetric Schiff base. Physicochemical cum spectroscopic characterization confirmed their formation. According to the molar conductance, both chelates are non-electrolytic in nature. Metal(II) chelates presented a coordination number of four by bonding to the H_2L ligand via its azomethine nitrogen atoms and phenolic oxygen atoms. The stoichiometry of the complexes derived from elemental analysis corresponds to 1:1 metal:ligand ratio. Several bacterial and fungal species have been examined for its biological activity, along with its chelates. Both chelates exhibited selective activity against the bacterial and fungal species. DPPH scavenging showed good activity of the compounds with CuL exhibiting the highest activity.

References

Abbas, S. Y., Darwish, S. A. and Aish, E. H. (2024). Synthesis of New Tetradentate H2salophen Ligands and Their

Copper(II) Complexes. *Egyptian Journal of Chemistry*, 67, SI: 655-660. https://dx.doi.org/10.21608/EJCHEM.2024.288342.9693

Abdel-Rahman, L. H., Adam, M. S. S., Al-Zaqri, N., Shehata, M. R., Ahmed, H. E. and Mohamed, S. K. (2022). Synthesis, Characterization, Biological and Docking Studies of ZrO(II), VO(II) and Zn(II) Complexes of a Halogenated Tetra-dentate Schiff Base. *Arabian Journal of Chemistry*, 15(5), 103737. https://doi.org/10.1016/j.arabjc.2022.103737

Abdel-Rahman, L. H., Al–Farhan, B. S., Al Zamil, N. O., Noamaan, M. A., Ahmed, H. E. and Adam, M. S. S. (2021). Synthesis, Spectral Characterization, DFT Calculations, Pharmacological Studies, CT-DNA Binding and Molecular Docking of Potential N, O-Multidentate Chelating Ligand and its VO(II), Zn(II) and ZrO(II) Chelates. *Bioorganic Chemistry,* 114, 105106. https://doi.org/10.1016/j.bioorg.2021.105106

Ahmed, S. K., Hussein, S., Qurbani, K., Ibrahim, R. H., Fareeq, A., Mahmood, K. A., Mohamed, M. G. (2024). Antimicrobial resistance: Impacts, challenges, and future prospects. *Journal of Medicine, Surgery, and Public Health*, 2, 100081. https://doi.org/10.1016/j.glmedi.2024.100081

Akbari, Z., Stagno, C., Iaci, N., Efferth, T., Omer, E. A., Piperno, A., Monazerozohori, M., Feizi-Dehnayebi, M. and Micale, N. (2024). Biological Evaluation, DFT, MEP, HOMO-LUMO Analysis and Ensemble Docking Studies of Zn(II) Complexes of Bidentate and Tetradentate Schiff Base Ligands as Antileukemia Agents. *Journal of Molecular Structure,* 1301, 137400. https://doi.org/10.1016/j.molstruc.2023.137400

Akter, N., Bourougaa, L., Mebarka, O., Ouassaf, M., Bhowmic, R. C., Uddin, K. M., Bhat, A. R. and Kawsar, S. M. A. (2024). Molecular Docking, ADME-Tox, DFT and Molecular Dynamics Simulation of Butyroyl Glucopyranoside Derivatives against DNA Gyrase Inhibitors as Antimicrobial Agents. *Journal of Molecular Structure,* 1307, 137930. https://doi.org/10.1016/j.molstruc.2024.137930

Bhuiyan, T.S., Said, M.A., Bulbul, M.Z.H., Ahmed, S., Bhat, A. R., Chalkha, M. and Kawsar, S. M. A. (2024). Synthesis, Antimicrobial and in silico Studies of C5′-O-substituted Cytidine Derivatives: Cinnamoylation Leads to Improvement of Antimicrobial Activity. *Nucleosides Nucleotides Nucleic Acids,* 43, 1472–1510. https://doi.org/10.1080/15257770.2024.2333495

Boulechfar, C., Ferkous, H., Delimi, A., Djedouani, A., Kahlouche, A., Boublia, A., Darwish, A. S., Lemaoui, T., Verma, R. and Benguerba, Y. (2023). Schiff Bases and their Metal Complexes: A Review on the History, Synthesis, and Applications. *Inorganic Chemistry Communications*, *150*, 110451. https://doi.org/10.1016/j.inoche.2023.110451

Czaplinska, B., Malarz, K., Mrozek-Wilczkiewicz, A., Slodek, A., Korzec, M., Musiol, R. (2020). Theoretical and Experimental Investigations of Large Stokes Shift Fluorophores Based on a Quinoline Scaffold. *Molecules*, 25(11), 2488. https://doi.org/10.3390/molecules25112488

Derafa, W., Moustafa, B. S., Mohamed, G. G., Taha, R. H. and Farhana, A. (2024). Design and Synthesis of a Novel Isoleucine-derived Schiff Base Ligand: Structural Characterization, Molecular Docking, and in vitro Biological Activity Evaluation. *International Journal of Health Sciences,* 18(6), 31 – 47.

Es-Sounni, B., Nakkabi, A., Bouymajane, A., Elaaraj, I., Bakhouch, M., Filali, F. R., El-Yazidi, M., El-Moualij, N. and Fahim, M. (2023). Synthesis, Characterization, Antioxidant and Antibacterial Activities of Six Metal Complexes Based Tetradentate Salen Type Bis-Schiff Base. *Biointerface Research in Applied Chemistry,* 13(4), 333. https://doi.org/10.33263/BRIAC134.333

Gacitúa, M.; Carreño, A.; Morales-Guevara, R.; Páez-Hernández, D.; Martínez-Araya, J.I.; Araya, E.; Preite, M.; Otero, C.; Rivera-Zaldívar, M. M.; Silva, A.; et al. (2022). Physicochemical and Theoretical Characterization of a New Small Non-Metal Schiff Base with a Differential Antimicrobial Effect against Gram-Positive Bacteria. *International Journal of Molecular Science,* 23, 2553. https://doi.org/10.3390/ijms23052553

GBD 2019 Antimicrobial Resistance Collaborators, Ahinkorah, B. O., Ali, S. S., Kandel, H., Kassa, B. G. and Shorofi, S. A. (2022). Global Mortality Associated with 33 Bacterial Pathogens in 2019: A Systematic Analysis for the Global Burden of Disease Study 2019. *The Lancet*, *400*(10369), 2221-2248. https://doi.org/10.1016/S0140-6736(22)02185-7

Geary, W. J. (1971). The Use of Conductivity Measurements in Organic Solvents for the Characterization of Coordination Compounds. *Coordination Chemistry Reviews*, 7: 81-122. https://doi.org/10.1016/S0010-8545(00)80009-0

Gogoi, H. P. and Barman, P. (2023). Salophen Type ONNO Donor Schiff Base Complexes: Synthesis, Characterization, Bioactivity, Computational, and Molecular Docking Investigation. *Inorganica Chimica Acta*, 556, 121668. https://doi.org/10.1016/j.ica.2023.121668

Hijazi, A. K., Taha, Z. A., Ajlouni, A M., Al-Momani, W. M., Idris, I. M., Hamra, E. A. (2017). Synthesis and Biological Activities of Lanthanide(III) nitrate Complexes with N-(2-hydroxynaphthalen-1-yl)methylene)nicotinohydrazide Schiff Base. *Medicinal Chemistry*, 13(1), 77–84. https://doi.org/10.2174/1573406412666160225155908

Hijazi, A. K., Taha, Z. A., Issa, D. K., Alshare, H. M., Al-Momani, W. M., Elrashidi, A. and Barham, A. S. (2024). Synthesis, Characterization and Catalytic/Antimicrobial Activities of Some Transition Metal Complexes Derived from 2-Floro-N-((2-Hydroxyphenyl)Methylene)Benzohydrazide. *Molecules,* 29, 5758. https://doi.org/10.3390/molecules29235758

Ilhan, S., Baykara, H., Seyitoglu, M. S., Levent, A., Özdemir, S., Dündar, A., Öztomsuk, A., Cornejo, M. H. (2014) Preparation, Spectral Studies, Theoretical, Electrochemical and Antibacterial Investigation of a New Schiff Base and its Some Metal Complexes. *Journal of Molecular Structure,* 1075, 32–42. https://doi.org/10.1016/j.molstruc.2014.06.062

Juyal, V. K., Thakuri, S. C., Panwar, M., Rashmi, P. O., Perveen, K., Bukhari, N.A. and Nand, V. (2024), Manganese(II) and Zinc(II) Metal Complexes of Novel Bidentate Formamide-based Schiff Base Ligand: Synthesis, Structural Characterization, Antioxidant, Antibacterial, and In-Silico Molecular Docking Study. *Frontiers in Chemistry,* 12, 1414646. https://doi.org/10.3389/fchem.2024.1414646

Kargar, H., Ardakani, A. A., Tahir, M. N., Ashfaq, M., Munawar, K. S. (2021). Synthesis, Spectral Characterization, Crystal Structure and Antibacterial Activity of Nickel(II), Copper(II) and Zinc(II) Complexes Containing ONNO Donor Schiff Base Ligands. *Journal of Molecular Structure,* 1233, 130112. https://doi.org/10.1016/j.molstruc.2021.130112

Mohamed, A. A., El-Gedamy, M. S., Sadeek, S. A., and Elshafie, H. S. (2025). First Report on some N_2O_2-Donor Sets Tetradentate Schiff Base and its Metal Complexes: Characterization and Antimicrobial Investigation. *Chemistry & Biodiversity*, 2025; 0:e01117 https://doi.org/10.1002/cbdv.202501117

Mohamed, A. A., Nassr, A. A., Sadeek, S. A., Rashid, N. G., Abd El-Hamid, S. M. (2023). First Report on Several NO-Donor Sets and Bidentate Schiff Base and Its Metal Complexes: Characterization and Antimicrobial Investigation. *Compounds*, 3, 376–389. https://doi.org/10.3390/compounds3030029

Mohapatra, D., Patra, S. A., Pattanayak, P. D., Sahu, G., Sasamori, T. and Dinda, R.

(2024). Monomeric Copper(II) Complexes with Unsymmetrical Salen Environment: Synthesis, Characterization and Study of Biological Activities. *Journal of Inorganic Biochemistry,* 253, 112497. https://doi.org/10.1016/j.jinorgbio.2024.112497

Nasaruddin, N. H., Ahmad, S. N., Sirat, S. S., Tan, K. W., Zakaria, N. A., Nazam, S. S. M., Abd Rahman, N. M. MYusof, N. S. M. and Bahron, H. (2022). Synthesis, Structural Characterization, Hirshfeld Surface Analysis and Antibacterial Study of Pd(II) and Ni(II) Schiff Base Complexes Derived from Aliphatic Diamine. *ACS Omega*, 7, 42809−42818. https://doi.org/10.1021/acsomega.2c04688

Soh, S. K. C., Assaw, S. and Zainuddin, N. A. (2023). Synthesis, Characterization of Copper(II) Complex with Tetradentate N2O2 and Potential Contribution as Promising Antibacterial Studies. *Universiti Malaysia Terengganu Journal of Undergraduate Research*, 5(2), 11-17. http://doi.org/10.46754/umtjur.v5i2.356

Nthehang, T. S., Waziri, I., Yusuf, T. L., Oselusi, S. O. and Muller, A. J. (2025). Synthesis, Structural Characterization, Biological and *In silico* Evaluation of Halogenated Schiff Bases as Potential Multifunctional Agents. *Journal of Molecular Structure* (2025), 1352(2), 144508. https://doi.org/10.1016/j.molstruc.2025.144508

Priya, J., Manimalathi, S. and Madheswari, D. (2024). Facile Synthesis, Spectral Characterization and Biological Evaluation of Metal Complexes Comprising ((1-Hydroxynaphthalen-2-yl) methyleneaminocyclohexylimino-methyl)naphthalen-1-ol Schiff Base Ligand and Assessing Chemo-pharmaceutical Properties. *Indian Journal of Chemistry,* 63, 211-225. https://doi.org/10.56042/ijc.v63i2.3515

Rajput, P., Nahar, K. S., and Rahman, K. M. (2024). Evaluation of Antibiotic Resistance Mechanisms in Gram-Positive Bacteria. *Antibiotics*, 13(12), 1197; https://doi.org/10.3390/antibiotics13121197

Russo, F., Vandelli, M., Biagini, G., et al., 2023. Synthesis and Pharmacological Activity of the Epimers of Hexahydrocannabinol. *Science Report,* 13 article s41598-023-32886-x

Singh, C., Adhikari, D. and K., Singh, B. K. (2024). Synthesis, Spectro-Thermal Characterization, DFT Calculations and Biochemical Evaluation of a Newly Synthesized Tridentate Schiff Base Transition Metal Complexes. *Polyhedron*, 259, 117050. http://dx.doi.org/10.2139/ssrn.4674352

Sogukomerogullari, H. G., Dede, B., Sahin, D. and Akkoç, S. (2025). Comprehensive Study on Synthesis, Quantum Chemical Calculations, Molecular Modeling Studies, and Cytotoxic Activities of Metal(II) Schiff Base Complexes. *Applied Organometallic Chemistry*, 39, e70034. https://doi.org/10.1002/aoc.70034

Wang, Y. P., Jiang, T. T., Wang, Y. C., Dong, H. X., Lu, J., Jin, J., Wang, W. L., Liu, Y. F. and Sun, J. (2024). Synthesis, Crystal Structure, Spectral Characterization and Antimicrobial Activity of Zn(II) and Ni(II) Compounds with the Schiff Base Ligand 3,5-dichlorosalicylaldehyde *o*-phenylenediamine. *Journal of Molecular Structure*, 1301, 137450. https://doi.org/10.1016/j.molstruc.2023.137450